NANO LETTERS

2007
Vol. 7, No. 1
211−217

Active Alignment of Microtubules with Electric Fields

Taesung Kim,[†] Ming-Tse Kao,[‡] Ernest F. Hasselbrink,[†] and Edgar Meyhöfer*[,†,‡]

Department of Mechanical Engineering, University of Michigan, 2350 Hayward Street, Ann Arbor, Michigan 48109, and Department of Biomedical Engineering, University of Michigan, 2200 Bonisteel Boulevard, Ann Arbor, Michigan 48109

Received June 26, 2006; Revised Manuscript Received October 30, 2006

ABSTRACT

The direction of translocation of microtubules on a surface coated with kinesin is usually random. Here we demonstrate and quantify the rate at which externally applied electric fields can direct moving microtubules parallel to the field by deflecting their leading end toward the anode. Effects of electric field strength, kinesin surface density, and microtubule translocation speed on the rate of redirection of microtubules were analyzed statistically. Furthermore, we demonstrated that microtubules can be steered in any desired direction via manipulation of externally applied E-fields.

Biomolecular motors are proteins that generate movement and forces in cells by interacting with cytoskeletal filaments (actin filaments or microtubules) and transducing chemical energy from the hydrolysis of adenosine triphosphate (ATP) into mechanical work. Single kinesin motors, for example, can generate ∼6 pN of maximum force by interacting with microtubules; surface-immobilized kinesins translocate microtubules in so-called in vitro assays with up to ∼50% efficiency[1] at a speed of about 0.8 μm/s via 8 nm steps.[2−4] Kinesins' nanoscopic size, low-energy consumption, and the high-energy storage density of ATP allude to the potential of biomolecular motors for nanotechnology applications, but substantial basic and engineering research remains to be done to realize this vision in a practical way. For example, we envision kinesin motors and microtubules as principal molecular transport mechanism for a variety of microdevices and Micro Total Analysis Systems (μTAS). To this end, we and others have demonstrated the first experimental implementations of molecular sorters on the basis of this concept.[5−7] In these devices, surface-immobilized kinesins serve as actuator to translocate microtubules that in turn act as handles for sorting and concentrating specific molecules. Unfortunately, the engineering of such a device is severely restricted because we currently lack the ability to precisely place kinesins into engineered device structures and to control their activity, speed, and directionality of motion along the microtubule. Interestingly, these technical challenges are directly mirrored by our limited understanding of how kinesin's activity is controlled in cells.[8] Consequently, most biomolecular motor-based applications focused on mechanically guiding kinesin-powered microtubules using passive techniques such as microchannel tracks[5,6,9−14] or a combination of structural and chemical patterns.[9,15] On the other hand, active mechanisms modulating biomolecular motor action will enhance the control and functionality of the proposed devices.

Recently, some progress has been made to direct biomolecular-motor-based transport and manipulate microtubules using electric fields.[5,7,16−21] Vassilev et al. first showed via electron microscopy that one can orient long bundles of microtubules parallel to the direction of electric fields,[19,20] and Stracke et al. characterized the electrophoretic mobility and charge density of tubulin by directly observing the motility of microtubules under constant electric fields.[17] Heuvel et al. increased the binding of microtubules from solution onto a kinesin-coated surface by applying electric fields normal to the surface via gold electrodes,[18] and Jia et al. and Heuvel et al. used electrophoretic and dielectrophoretic forces to selectively sort kinesin-transported microtubules that approached a bifurcation junction.[5,7] Parallel alignment of actin filaments with weak electric fields on a myosin-coated surface was demonstrated by Riveline et al.[16] On the other hand, several previous studies employing electric fields have been unsuccessful in manipulating microtubule-based motility for reasons that remain unclear.[5,17] For example, previous work attributed the poor response of microtubules to weak electrophoretic forces,[5,17] These forces were not able to noticeably deflect the relatively rigid microtubules, which have flexural rigidity almost 3 orders

* Corresponding author. Edgar Meyhöfer, University of Michigan Department of Mechanical Engineering, 2350 Hayward St, Ann Arbor, MI 48109. E-mail: meyhofer@umich.edu. Voice: (734) 647-7856. Fax: (734) 615-6647.

[†] Department of Mechanical Engineering.

[‡] Department of Biomedical Engineering.

10.1021/nl061474k CCC: $37.00 © 2007 American Chemical Society
Published on Web 12/08/2006

of magnitude stiffer than that of actin filament.[22,23] Other possible explanations for the weak responses of microtubules to electric fields include high kinesin densities, electroosmotic flow, Joule heating of solutions, and pH changes and oxygen generation associated with hydrolysis of the physiological buffer.

The goal of our work was to systematically explore the use of electric fields to actively control the direction of microtubule transport in in vitro motility assays. We demonstrate that kinesin-powered microtubules can in fact be rapidly redirected by modest electric fields. Direct fluorescence microscopy observations of the deflection dynamics of single microtubules and the statistical properties of many individual microtubule steering events strongly support the hypothesis that the leading end of microtubules acts as a free cantilever beam that turns toward the anode. As a microtubule is translocated forward by bound kinesins, the length of the unbound, leading end and its mean deflection due to the electrophoretic force on the negatively charged microtubule increases continuously. Binding to the next kinesin located along the microtubule's path preserves the mean deflection and leads to the turning of the microtubule. This mechanism is consistent with our experimental observations that the rate of microtubule redirection depends on the kinesin surface density and translocation velocity.

To study the effect of electric fields on kinesin-based microtubule gliding, we constructed test chambers from 0.17 mm thick cover glasses (Corning, Corning NY) using strips of 75 μm thick double-sided tape (Tesa 5338, Beiersdorf, Hamburg, Germany) as spacer. Prior to bonding of the cover glasses, the inner edges of the tape were sealed with vacuum grease to prevent leakage of glue solvents into the motility buffer. The resulting channels had dimensions of approximately 4 mm by 0.075 mm in cross section. At each end of the channels we mounted and sealed small glass pipet tips with UV-epoxy (NOA68, Norland, NJ) to serve as access ports and reservoirs to the microchannel. Clean, bright platinum electrodes (99.9%), connected to a dc power supply (E3612A, Agilent Technologies, Palo Alto, CA), were inserted into the reservoirs to apply electric fields ranging from 0 to 250 V. We carefully monitored the pH of the motility buffer in the reservoirs when applying electric fields to the channels to avoid adverse effects on the microtubule motility due to the electrolysis of water.

For most experiments we used a bacterially expressed kinesin motor, NKHK560cys. This motor consists of the head and neck domain of *Neurospara crassa* kinesin (amino acids 1−433) and the stalk of *Homo sapiens* kinesin (residues 430−560) and a reactive cysteine at the C-terminal end.[24] NkHK560 was expressed and purified as described previously.[14,25] To estimated the surface density of kinesin in our assays, we labeled the reactive, C-terminal cysteine of our kinesin construct with Cy3 (GE Healthcare, Piscataway, NJ) and characterized the labeling stoichiometry from the known molar extinction coefficient of the dye using a spectrophotometer (Biospec 1601, Shimadzu, Columbus, MD).[25] The fluorescence intensity of individual kinesin molecules was estimated from the stepwise photobleaching behavior of single kinesin motors and the Cy-3 labeling ratio. In addition, we conducted some control experiments with tissue-purified bovine kinesin, which was isolated by microtubule affinity and gel filtration chromatography. Tubulin was purified from cow brain by three cycles of microtubule polymerization and depolymerization followed by phosphocellulose ion exchange chromatography, and fluorescently labeled tubulin (TMR-tubilin) was prepared by reacting polymerized microtubules with a 20-fold excess of tetramethylrhodamine (Molecular Probes) at room temperature for 30 min. Competent, labeled tubulin was purified from this mixture by repeated depolymerization and polymerization. For all experiments, microtubules were polymerized by incubating 2 mg/mL tubulin (equal ratios of TMR-labeled and unlabeled tubulin), 1 mM GTP, and 4 mM $MgCl_2$ in BRB80 buffer at 37 °C for 20 min. Microtubules were stabilized by the addition of 10 μM taxol. All motility assays were carried out in BRB80 buffer at pH 6.8 at room temperature.

Gliding assays were performed by introducing 100 μL of 6.9 μM kinesin in a casein−BRB80 solution into the test cells and allowing it to incubate for 5 min, followed by flushing with 100 μL of motility buffer containing rhodamine-labeled microtubules at a final concentration of 30 μg/mL tubulin. For lower density motility assays, we reduced the kinesin concentration 10-fold to about 0.69 μM. Using Cy3-labeled kinesin and quantitative fluorescence microscopy, we estimated the kinesin surface density to be about 25000 and 2500 molecules/μm^2 for the high and low density assays, respectively. All fluorescence experiments and motility assays were carried out with an Axiovert 200 inverted microscope (Carl Zeiss Microimaging, New York) equipped with a digital CCD camera (Orca ER II, Hamamatsu, Japan). Both high and low kinesin concentrations resulted in motility assays supporting continuous, uninterrupted long distance transport of microtubules, while further dilution of kinesin yielded intermediate density assays characterized by discontinuous microtubule gliding as expected on the basis of previous work (for example, refs 1−5 and 25). In the absence of electric fields (Figure 1a), microtubules translocate in random directions. However, as soon as the electric field is applied (Figure 1b), microtubules start to turn toward the anode and align with the direction of electric fields (Figure 1c). After 30 s, nearly all the microtubules are translocating roughly parallel to the electric field toward the anode.

To determine the influence of the kinesin surface density and electric field strength on the turning behavior of microtubules, we compared the alignment of microtubules in electric field experiments at low and high kinesin densities and as a function of electric field strength. Snapshots of motility assays 30 s after the different electric fields were switched on (Figure 2) show that the turning behavior of microtubules is strongly influenced by the electric field strength and kinesin surface density. Microtubules redirect faster at higher field strength (Figure 2d,h) and lower kinesin density (Figures 2b−d). These data suggest that the observed alignment process of microtubules is due to electrophoretic (Coulombic) forces, which is in agreement with previous reports suggesting that microtubules contain at least −280*e*

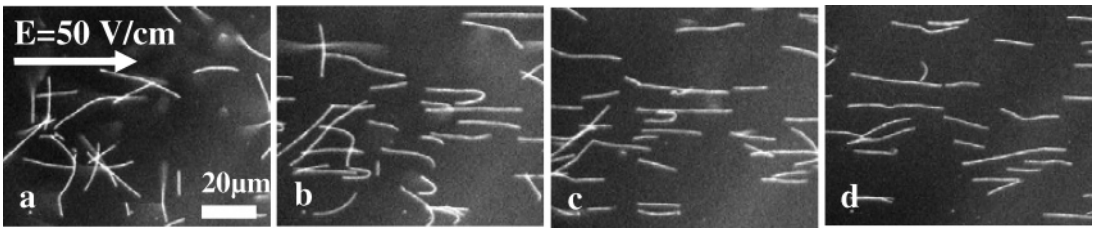

Figure 1. Directional response of kinesin-based microtubule transport to electric fields. Following the application of an electric field of 50 V/cm, a series of images (a through d) was recorded at 10 s time intervals. At the lower kinesin surface densities (0.69 μM kinesin in the incubation buffer) continuous application of electrophoretic force rapidly redirects microtubules parallel to the electric field.

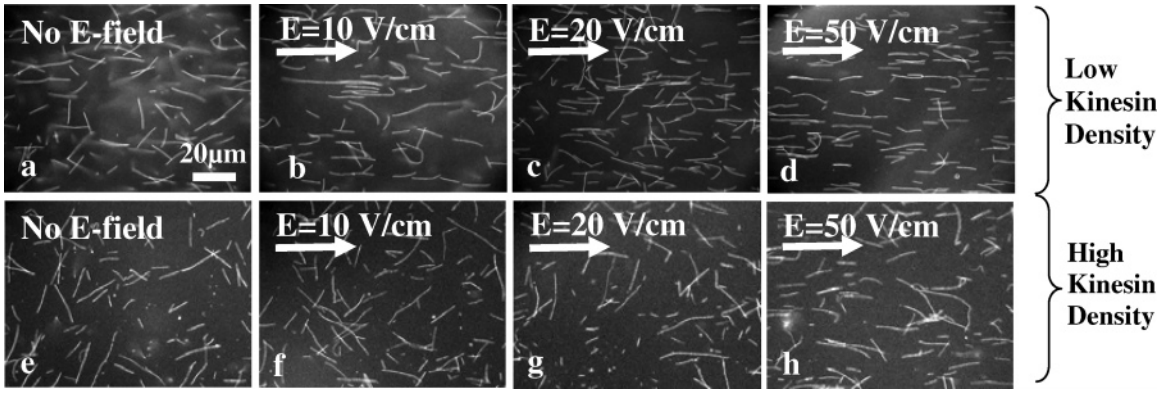

Figure 2. Gliding assay response to the application of various electric fields. (a) Low kinesin concentration, no electric field (standard gliding assay). (b−d) Low-density kinesin gliding assays after 30 s exposure to electric fields of 10, 20, and 50 V/cm, respectively. (e) High kinesin concentration, no electric field (standard gliding assay). (f−h) High concentration kinesin gliding assays, after 30 s exposure to electric fields of 10, 20, and 50 V/cm, respectively.

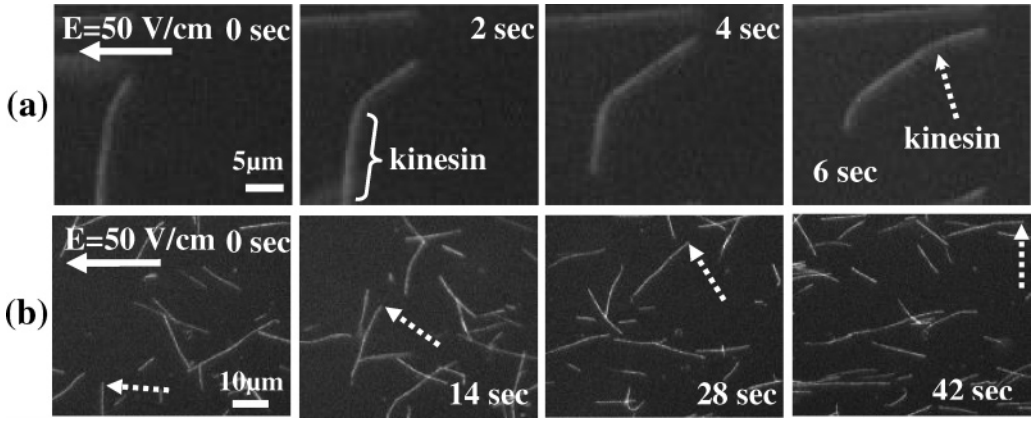

Figure 3. Sequences of microtubule alignment at different concentrations of kinesin in the presence of electric fields. (a) A microtubule turning event at a low density of kinesin. The free, leading end of the microtubule makes a sharp turn prior to its apparently binding to another kinesin. (b) A microtubule redirection event in a high-density kinesin assay. The turn of the microtubule is slower and more gradual.

of charge per micrometer of length.[17,26] Moreover, it is also unlikely that electrophoretic forces could detach a microtubule from surface-bound kinesin molecules because the electrophoretic force F_{EP} per unit length of microtubules that can be calculated as $F_{EP} = q'_{MT}E$ ($F_{EP} = 0.2$ pN/μm, where $q'_{MT} = -280$e/μm is the linear charge density[17] and $E = 50$ V/cm is the strength of an electric field) is far less than the maximum force that may be exerted by even a single kinesin on a microtubule (about 6 pN/kinesin[2,3]).

Further qualitative support for the mechanism and rate of microtubule alignment can of course be gained by observing the deflection and movement trajectories of individual microtubules at different kinesin surface densities (Figure 3). A representative microtubule deflection event at the lower kinesin surface density is shown in Figure 3a. As the microtubule continues to translocate upward, its leading end is observed to experience significant bending to the right due to the presence of a nearly perpendicular electric field of strength 50 V/cm. We interpret this sequence as follows: During the initial phase of this microtubule redirection event (interval between 0 and 2 s) a several micrometer-long portion of the leading end of the microtubule transiently detached from the kinesin-coated surface. This cantilevered portion of the microtubule was then appreciably deflected

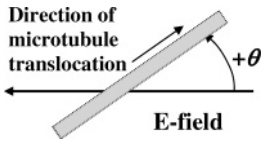

Figure 4. Definition of microtubule translocation direction θ_i ($-180 < \theta_i < 180$). Counterclockwise is positive.

by the electrophoretic forces acting on the microtubule before the leading end of microtubule re-engaged with surface-bound kinesins in the deflected orientation. The leading end of the microtubule, supported by the interaction with multiple kinesins, continued to move in a relatively straight path ($t = 4$ s), while the microtubule deflection is maintained in a single bend of radius $\sim 4\ \mu$m. A few seconds later ($t = 6$ s) another, but more gradual, deflection event is visible. In high kinesin assays, on the other hand, the alignment process is much more gradual (Figure 3b). The microtubule indicated with a dotted-arrow in Figure 3b turns smoothly, with a large radius of curvature ($r > 50\ \mu$m).

Clearly, the observed turning behavior of microtubules relates both to the applied electric field and to the kinesin-based microtubule transport. While the electric field applies a uniform transverse load, we do not expect that the microtubule is supported uniformly at all times, largely because the kinesin motors on the glass surface are randomly and locally nonuniformly oriented. Thus, while translocating, the leading end of microtubules will be cantilevered beyond its kinesin supports at various length that continuously fluctuate. The cantilevered portion of the microtubule may then be deflected toward the anode, until the tip is engaged by another kinesin and the process repeats. When the leading tip of the microtubule moves from kinesin to kinesin, it deflects by some (small) amount until it is eventually aligned with the electric field. Since the deflection of a cantilever subjected to a uniform load is proportional to the load force and the fourth power of the length of the cantilever, this hypothesis predicts that the rate of microtubule alignment should be faster at higher electric fields and slower at higher surface density of active kinesin. This working hypothesis also predicts, in agreement with the experimental observations in Figure 3a, that the alignment of microtubules will not be entirely smooth, rather a few individual microtubule defection events of the longest cantilevered leading microtubule portions will dominate the turning behavior, because of the fourth power length dependence of the microtubule deflection. Last, we expect that the rate of microtubule alignment should be increased with increasing translocation speed.

To quantitatively test these predictions, we examined the behavior of redirected microtubules statistically. In order to quantify the rate of microtubule alignment, we employed a straightforward image processing technique and determined, as shown in Figure 4, the angle between the leading end of a microtubule in each video frame and the direction of the applied electric field. Translocation direction θ_i is defined as the angle between the negative of the electric field vector and a vector pointing in the direction of microtubule translocation.

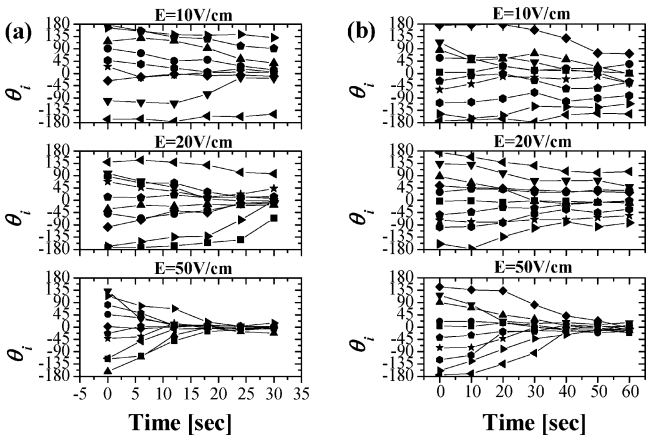

Figure 5. Individual microtubule directions θ_i vs time. (a) Low kinesin surface density at various electric fields. θ_i for 10 cases are shown. (b) High kinesin surface density.

Sample histories of θ_i for ensembles of 10 randomly selected microtubules are plotted for these three applied electric fields in Figure 5. In all cases, it is apparent that the electric field aligns all microtubules, but at lower kinesin surface densities (Figure 5a), the alignment is more pronounced and occurs much faster than that in the high-density cases (Figure 5b). We also note that the trend toward aligning is *not* monotonic: some microtubules will briefly become less aligned, suggesting that random events (e.g., thermal energy, kT, and fluctuations or energy, where k is Boltzmann constant and T is absolute temperature) play a strong role in individual microtubule translocation kinematics.

In order to attain statistical data, we obtained ensemble-averaged statistics for $N = 50$ microtubules as a function of time. Of course, for an infinite sample size, both randomly oriented microtubules and perfectly aligned microtubules have an average orientation equal to $\theta_{avg} = 0°$. However, the root-mean-square (rms) value of the angle (θ_{rms}) is equal to $\theta_{rms} = (\pi^2/3)^{1/2} = 103.9°$ for randomly oriented microtubules, while an ensemble of perfectly aligned microtubules will have $\theta_{rms} = 0.0°$. Therefore, we choose θ_{rms} as a convenient measure of statistical alignment, calling this statistically obtained value the "directionality".

Values of θ_{rms} ($N = 50$) were obtained from individual frames of long video sequences and plotted as functions of time for different electric field strengths and kinesin surface densities (Figure 6). Figure 6a shows the statistical analysis of the directionality of microtubules at low concentration of kinesin (corresponding to panels a−d of Figure 2). The θ_{rms} before electric fields are applied is close to 103.9°, as expected (error bars include sampling as well as estimated measurement errors). After electric fields are applied, θ_{rms} decreases with time and, consistent with Figure 2, the rate of redirection is larger under higher electric fields. Figure 6b shows the result at identical conditions, except that motility conditions with high kinesin surface densities were used (corresponding to panels e−h of Figure 2). Consistent with our cantilever-beam deflection hypothesis, θ_{rms} decreases significantly faster at low concentrations of kinesin than at high concentration when comparing results at similar electric fields. Notice, however, that the root-mean-square

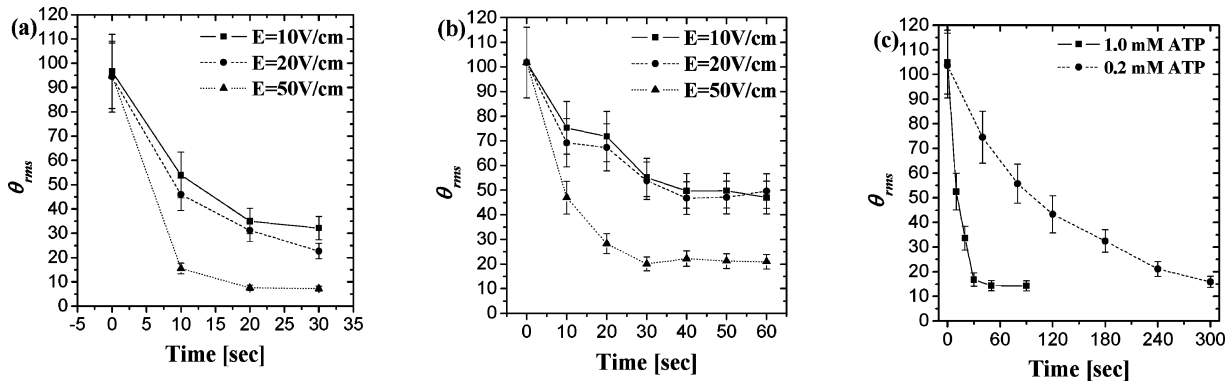

Figure 6. Directionality (θ_{rms}) of microtubules vs time ($N = 50$) at low (a) and high (b) kinesin surface densities and as a function of ATP concentration (c) in the presence of a 50 V/cm E-field.

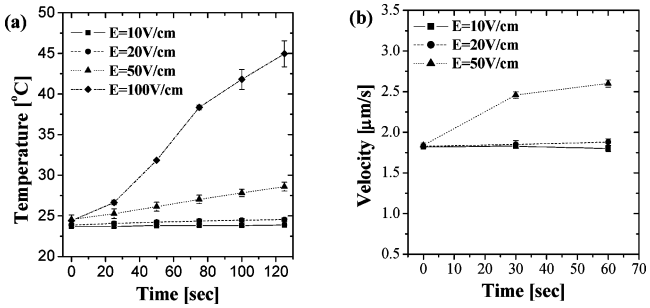

Figure 7. Temperature of the buffer solution at the cathode side of the reservoir measured with a thermocouple under various ranges of electric fields (a). The gliding velocities of microtubules on low concentration of kinesin are shown in (b).

value of the microtubule translocation direction approaches asymptotically nonzero values, especially at higher kinesin surface densities. In addition, we investigated the rate of redirection of microtubules translocating in physiological buffer solutions with different ATP concentrations (Figure 6c). In agreement with our general working hypothesis, microtubules moving slower (0.36 ± 0.17 μm/s) at limiting ATP concentrations (0.2 mM) turned significantly less rapidly than fast moving microtubules (1.58 ± 0.14 μm/s) at saturating ATP concentrations (1 mM).

While the data in Figure 6 strongly argue that the electric field strength controls the alignment rate of microtubules, we were concerned that this might not be a direct effect that electric fields exert on microtubules. One such possibility is that higher electric field strengths might cause significant Joule heating of the physiological assay buffer. Furthermore, it is well-known that, for example, an increase in temperature from 20 to 40 °C will increase the microtubule gliding speed about 5-fold,[27−29] and since our cantilever hypothesis predicts that the microtubule redirection rate depends on the translocation speed, the observed fast redirection of microtubules, particularly at 50 V/cm, might be due to a Joule-heating-based temperature increase in the test chamber. Therefore, we characterized the temperature increase in the test chamber and translocation speed of the microtubules as a function of time at three electric field strengths (Figure 7). Clearly, at $E = 50$ V/cm there is a noticeable increase in temperature and concomitant increase in microtubule translocation speed, which is in good agreement with results of previous work. However, it is also clear that this temperature increase is significantly delayed relative to the alignment of microtubules (compare Figures 6 and 7), and thus we reject the hypothesis that Joule heating is major factor responsible for the faster alignment of microtubules at higher field strength. On the other hand, the data for $E = 100$ V/cm in Figure 7a show that large electric fields (in test chambers with dimensions comparable to ours field strength in excess of ~ 50 V/cm) can readily lead to temperature changes that will need to be considered in quantitative models or even irreversible denature proteins. In our experiments, motility ceased within a few minutes when fields of 100 V/cm were applied, presumably as a result of excessively high temperatures.

An important quantitative aspect of our data relates to question of why electric-field-aligned microtubules approach asymptotic nonzero values for the root-mean-square angular direction. And why should the asymptotic values be larger for the high-density kinesin cases? We believe that this average behavior is due to random, thermal fluctuations of a leading microtubule tip, which prevents microtubules from aligning perfectly with the applied electric field. These fluctuations are also responsible for the slow directional change in microtubule gliding assay in the absence of electric fields. Our simple cantilever-beam deflection hypothesis does not include these random effects and therefore does not predict this observed nonzero asymptotic directionality. During microtubule transport when some length ΔL of a microtubule tip becomes cantilevered over a certain distance without support, Gittes et al. show that the fluctuations of the tip due to Brownian motion are expected to scale as $(\Delta L^3 kT)^{1/2}$.[30] At the same time, the steady deflection due to the electric field is expected to scale as (ΔL).[4] Thus, when ΔL is shorter (high kinesin density cases), one expects the relative importance of random fluctuations to actually be more important than when ΔL is longer. Thus, we expect the equilibrium θ_{rms} to be larger in the higher kinesin density cases, and conversely, we expect electrophoretic forces to be more important at larger ΔL to drive the leading end of the microtubule more effectively to zero angle asymptotic directionalities.

In conclusion, our direct experimental observations and the quantitative data presented here appear only consistent with the beam-deflection hypothesis, and other models that

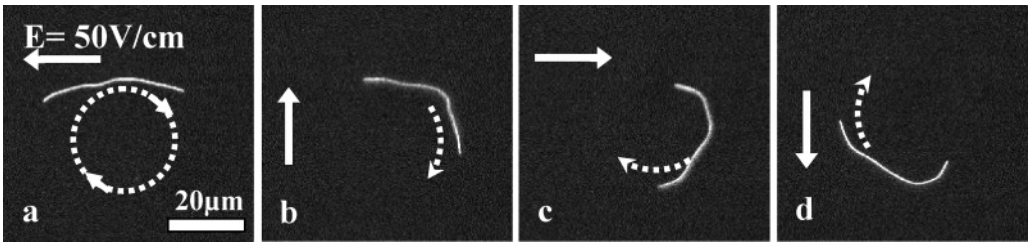

Figure 8. Applying an electric field that is rotating in time produces circular translocation of a microtubule. Voltages are applied at four reservoirs at the corners of a square microfluidic chamber (not shown) to rotate the electric field as shown by the solid arrows. In (a), the microtubule is initially translocating to the right; the dotted circle in (a) shows an approximate desired microtubule trajectory. By changing the electric field upward in panel b, the microtubule starts to translocate downward. Continued rotation of the electric field guides the microtubule leftward (c) and upward (d).

we considered (such as the possibility of an aligning torque, caused by charge differences at the plus and minus ends of the microtubule) have been largely discounted. Since the proposed mechanism for the electric-field-based alignment of moving microtubules is entirely based on a direct physical interaction of the electric field with the charged microtubules that are transported by surface immobilized kinesins, an important inference from our work is that the type of kinesin is not important in its own right but that the surface density and speed of translocation of kinesins influence the rate of alignment. We therefore conducted a series of control experiments with tissue-purified, full-length bovine kinesin which is well-known to adsorb at higher surface densities (compared to truncated kinesins) to standard glass substrates via the numerous, nonspecific interactions of the stalk and tail domain. When we repeated the above experiments, we observed that bovine kinesin behaved identical with NKHK560: microtubules translocating at low surface density conditions aligned more rapidly than those moving in high density assays. However, there was a very important difference: microtubules turned very poorly at the highest densities and usually 10−30-fold nominal dilutions were required to match the alignment behavior of assay using truncated NKHK560 kinesin. These control experiments on bovine kinesin further support our cantilever-beam deflection hypothesis and suggest that the kinesin density is a key factor in the quantitative behavior of electric-field-based microtubule alignment. In addition, the slower speed of bovine kinesin (~0.8 μm/s compared to ~1.8 μm/s)[31] is likely to contribute to the observed rates of microtubule alignment. Our comparative experiments with NKHK560 using saturating and limiting ATP concentrations to alter the gliding speed of microtubules (Figure 6c) directly support this view. Taken together, our work implies that, in addition to the strength of the electric field and the kinesin surface density, the translocation speed is an important determinant of the rate of microtubule alignment in electric fields. Furthermore, our experimental observations resolve some experimental differences by suggesting that the relatively poor alignment of microtubules in a number of previous reports (for example, ref 17) is likely due to the weaker electric fields (12.5 vs 50 V/cm) and higher kinesin density.

Last, we wanted to demonstrate the flexibility that electric-field-based steering offers over previously reported, passive methods and demonstrate that it is indeed feasible to exert real-time directional control over moving microtubules. We directed microtubules to translocate in ~30 μm diameter circles (Figure 8) by manipulating the electric field through voltages on order of 50 V/cm applied at four reservoirs around the periphery of the device. Our control over the directional movement of microtubules is comparable in resolution to that first achieved by Hiratsuka et al. who used passive structures to mechanically guide microtubules,[13] but our electric-field-based directional control method offers the significant advantage of active, real-time control over the microtubule movement.

Biomolecular motor and microtubule-based nanoscale transport mechanisms offer significant advantages, including their nanoscopic size, high efficiency, and substantial force, directional control of microtubules, that open up unique functional capabilities and suggest intriguing micro- and nanodevice applications (see for example refs 6, 7, and 10−15). The method of employing electric fields as presented in this paper not only makes it much easier to build molecular motor-powered μTAS systems by reducing microfabrication typically required in manufacturing passive guide patterns but also enables highly flexible, configurable control over the direction of actively and continuously moving microtubules in nanotransport systems.

Acknowledgment. This work has been supported by DARPA Contract N66001-02-C-8039 and NSF Grant No. BES 0428090.

Supporting Information Available: Movies documenting (1) the rapid alignment of microtubules in response to an electric field and (2) active directional control of transport by continuously redirecting microtubules into a circular pattern. This material is available free of charge via the Internet at http://pubs.acs.org.

References

(1) Howard, J. *Annu. Rev. Physiol.* **1996**, *58*, 703−729.
(2) Hunt, A. J.; Gittes, F.; Howard, J. *Biophys. J.* **1994**, *67* (2), 766−781.
(3) Meyhofer, E.; Howard, J. *Proc. Natl. Acad. Sci. U.S.A.* **1995**, *92* (2), 574−578.
(4) Schnitzer, M. J.; Block, S. M. *Nature* **1997**, *388* (6640), 386−390.
(5) Jia, L. L.; Moorjani, S. G.; Jackson, T. N.; Hancock, W. O. *Biomed. Microdevices* **2004**, *6* (1), 67−74.
(6) Kim, T. S.; Nanjundaswamy, H. K.; Lin, C.-T.; Lakämper, S.; Cheng, L. J.; Hoff, D.; Hasselbrink, E. F.; Guo, L. J.; Kurabayashi, K.; Hunt, A. J.; Meyhöfer, E. *μ-TAS* **2003**, *1*, 33−36.

(7) van den Heuvel, M. G. L.; De Graaff, M. P.; Dekker, C. *Science* **2006**, *312* (5775), 910−914.
(8) Verhey, K. J.; Rapoport, T. A. *Trends Biochem. Sci.* **2001**, *26* (9), 545−550.
(9) Cheng, L. J.; Kao, M. T.; Meyhofer, E.; Guo, L. J. *Small* **2005**, *1* (4), 409−414.
(10) Clemmens, J.; Hess, H.; Howard, J.; Vogel, V. *Langmuir* **2003**, *19* (5), 1738−1744.
(11) Clemmens, J.; Hess, H.; Matzke, C.; Bachand, G.; Bunker, B.; Vogel, V. *Biophys. J.* **2003**, *84* (2), 293A−293A.
(12) Dennis, J. R.; Howard, J.; Vogel, V. *Nanotechnology* **1999**, *10* (3), 232−236.
(13) Hiratsuka, Y.; Tada, T.; Oiwa, K.; Kanayama, T.; Uyeda, T. Q. P. *Biophys. J.* **2001**, *81* (3), 1555−1561.
(14) Lin, C. T.; Kao, M. T.; Kurabayashi, K.; Meyhofer, E. *Small* **2006**, *2* (2), 281−287.
(15) Clemmens, J.; Hess, H.; Lipscomb, R.; Hanein, Y.; Bohringer, K. F.; Matzke, C. M.; Bachand, G. D.; Bunker, B. C.; Vogel, V. *Langmuir* **2003**, *19* (26), 10967−10974.
(16) Riveline, D.; Ott, A.; Julicher, F.; Winkelmann, D. A.; Cardoso, O.; Lacapere, J. J.; Magnusdottir, S.; Viovy, J. L.; Gorre-Talini, L.; Prost, J. *Euro. Biophys. J. Biophys. Lett.* **1998**, *27* (4), 403−408.
(17) Stracke, R.; Bohm, K. J.; Wollweber, L.; Tuszynski, J. A.; Unger, E. *Biochem. Biophys. Res. Commun.* **2002**, *293* (1), 602−609.
(18) van den Heuvel, M. G. L.; Butcher, C. T.; Lemay, S. G.; Diez, S.; Dekker: C. *Nano Lett.* **2005**, *5* (2), 235−241.
(19) Vassilev, P.; Dronzin, R.; Kanazirska, M.; Georgiev, G. *Stud. Biophys.* **1982**, *90*, 111−112.
(20) Vassilev, P. M.; Dronzine, R. T.; Vassileva, M. P.; Georgiev, G. A. *Biosci. Rep.* **1982**, *2* (12), 1025−1029.
(21) Kim, T. S.; Kao, M.-T.; Hasselbrink, E. F.; Meyhofer, E. *μ-TAS* **2005**, *1*, 1234−1236.
(22) Gittes, F.; Mickey, B.; Nettleton, J.; Howard, J. *J. Cell Biol.* **1993**, *120* (4), 923−934.
(23) Mickey, B.; Howard, J. *J. Cell Biol.* **1995**, *130* (4), 909−917.
(24) Lakamper, S.; Kallipolitou, A.; Woehlke, G.; Schliwa, M.; Meyhofer, E. *Biophys. J.* **2003**, *84* (3), 1833−1843.
(25) Lakamper, S.; Meyhofer, E. *Biophys. J.* **2005**, *89* (5), 3223−3234.
(26) Nogales, E.; Wolf, S. G.; Downing, K. H. *Nature* **1998**, *393* (6681), 191−191.
(27) Bohm, K. J.; Stracke, R.; Baum, M.; Zieren, M.; Unger, E. *FEBS Lett.* **2000**, *466* (1), 59−62.
(28) Kawaguchi, K.; Ishiwata, S. *Biochem. Biophys. Res. Commun.* **2000**, *272* (3), 895−899.
(29) Mazumdar, M.; Cross, R. A. *J. Biol. Chem.* **1998**, *273* (45), 29352−29359.
(30) Gittes, F.; Mickey, B.; Howard, J. *FASEB J.* **1992**, *6* (1), A27−A27.
(31) Steinberg, G.; Schliwa, M. *Mol. Biol. Cell* **1995**, *6* (11), 1605−1618.

NL061474K